Landslide susceptibility modeling using the weight of evidence approach: case of Al Hoceima city (Northern Morocco)

Taoufik BYOU

Department of Geography, Laboratory Dynamics of Arid Environments, Regional Planning and Development.

Mohammed Premier University, BV Mohammed VI BP:524, 60000 Oujda, Morocoo.

Corresponding author: taoufikbyou@gmail.com

Abstract. The Rif mountains in northern Morocco experience frequently geomorphological hazards, including landslides that hamper urban management.This paper aims to develop an objective approach for the assessment of landslide susceptibility in the city of Al Hoceima based on a bivariate probabilistic model (weight of evidence). This approach allows analyzing the relationships between the spatial occurrence of landslides and the different natural and anthropogenic parameters that tend to accentuate and aggravate the formation of this phenomenon. The purpose of our work is landslide hazard zoning while ensuring a better zoning of the landslide susceptibility with a good prediction. The results of the Receiver Operating Characteristic (ROC) curve show that the comparison of the preferred landslide susceptibility map with the inventory map gives a good predictive capability (AUC= 0.902). The obtained map shows that high to very high susceptibility zones contain 69% of the total landslides inventoried. The mapping products of this work can be considered as a major contribution to the elaboration of urban development plans in the city of Al Hoceima.

Keywords: GIS, weight of evidence, Landslide susceptibility assessment, Al Hoceima (Morocco)

INTRODUCTION

The Rif mountain range is known as an area exposed to landslides due to its rugged relief, geological structure and climatic conditions. These conditions damage the infrastructure and handicap the sustainable development of the region. The city of Al Hoceima, situated to the north of the Rif chain on the Mediterranean coast, is the area most affected by landslides. This phenomenon is rather precarious as many landslides occur there frequently during rainy periods. The rainfall which occurred in recent decades in Al Hoceima region has highlighted the vulnerability to landslide phenomena. This vulnerability is increasing due to the intensification of land use and socio-economic development. The population growth rate increased relatively during the period 2004-2014, at 0.25% against 0.1% at the national level. This is due to the internal emigration of populations from the rural communes to Al Hoceima city. Most of them built their houses in areas not suitable for construction near rivers or in unstable areas. This makes the mapping of landslide susceptibility a high priority in this area to guide the future development of urbanization and mitigate damages.

Numerous works have been devoted to the spatial evaluation of the randomness linked to ground movements in the Rif: Millies-Lacroix (1968) drew up, for the Rif as a whole, a forecast map of ground movements at

1/1000000. This map integrates five main factors: lithology, topography, climate, vegetation, anthropogenic action. In the central Rif, Maurer (1968) was mainly interested in the mapping of landslides, particularly those of a superficial nature. Then, Fares (1994) and Margaa (1994) used the ZERMOS (Risk-mapping of areas exposed to movements of soil) mapping methods in Taounate and Al Hoceima regions respectively. These methods are based on the evaluation of the role of each of the permanent factors retained. Hazard zoning was established based on the combination of these permanent factors and their prioritization according to the degree of potential risk.

The objective of this work is to assess the susceptibility to landslides based on a bivariate statistical model, based on Bayes theorem (weight of evidence)(Spiegelhater and Kill-Jones, 1984). The potentiality of this model derives from its reproducible objective character and the fact that it quantifies the probability of landslide occurrence. The analysis of the accuracy of the model is performed by the ROC (Receiver Operating Characteristic) curve by comparing the inventory map and the obtained susceptibility map.

In this work we present a diagnostic of landslides occurring in the area of study through their inventories, mapping, and characterization. Then, we develop a database integrating the causative factors of landslides to help performing calculation and interpretation of the weighted factors used in this analysis. The final results of landslide susceptibility map are validated using the AUC (Area Under the Curve) criterion.

The town of Al Hoceima is located in the eastern part of the Bokkoya massif of the Rif mountains in northern Morocco and is spread over an area of 34 km2. It is made up of incised valleys, separated by landforms strongly sloping which are marked by limestone ridges reaching 406m at Jbel Monte Pamomas, 300m at Jbel Malmusi, and by high cliffs that often exceed 100 m at the level of the dolomitic plateaus "Morro nuevo". The east of Al Hoceima is dominated by irregular slopes of fairly soft shapes, bordering the sea with an altitude higher than 130 m (Figure 1).

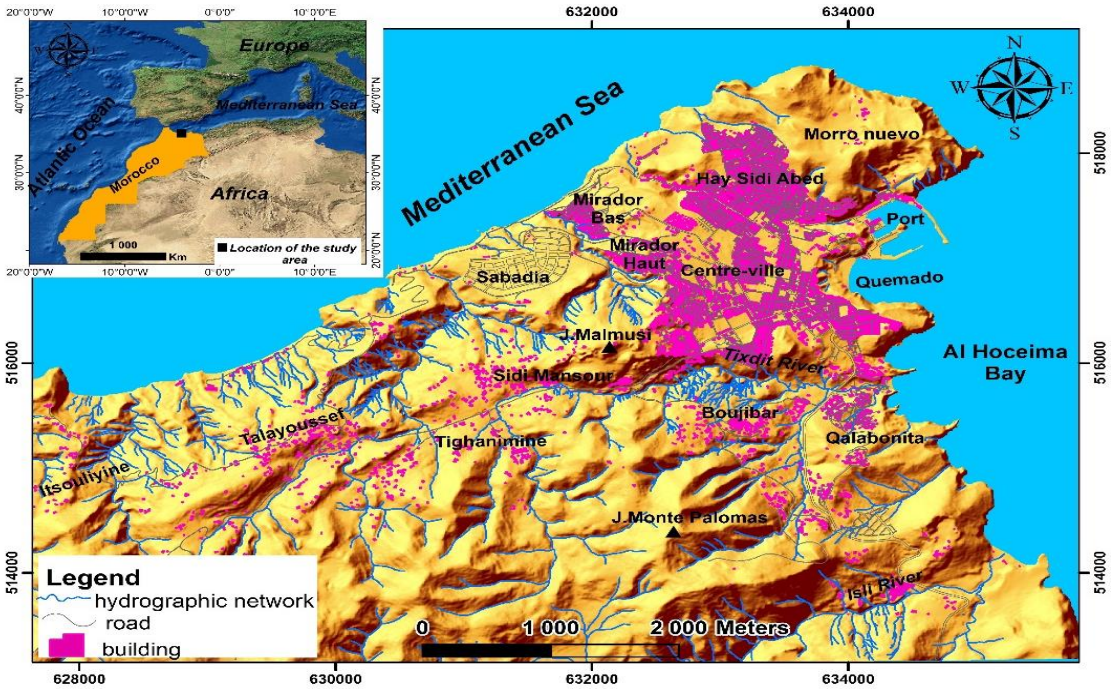

Figure 1: Situation of the city of Al Hoceima (restitution plan, scale 1/2000)

Geologically, the study area is formed by thrust/nappe complex as such is the case of the entire Rif belt. More particularly, The Al Hoceima region is characterized by the stacking of four structural nappes separated by anomalous contactsput in place starting from the Late Oligocene, (Figure 2): (1) The Boussecour nappe, formed by Triassic dolomites and flint limestones, (2) The Eo-Oligocene nappe, consisting mainly of marl formations. (3) The Al Hoceima nappe, constituted by the Primary materials including Silurian shales, Devonian limestones, sandstones, and Permo-Triassic argillites. These materials are superimposed on the previous nappes in the form of Klippe. This Klippe extends from Al Hoceima to Boussekkour valley in the west. (4) The Jbel Amekrane nappe formed by the Lias limestones, known for their white color. The outcrop of this nappe at Jbel Palemas surmounts the previous nappes in the form of Klippe. The whole, constituting the Bokkaya massif, overthrust towards the south on the Tisirene flysch. The Eo-Oligocene nappe being the Tertiary sole. (Mégard, 1963; Andrieux, 1971, Mourier, 1982; Azzouz, 1992).

The region is characterized by a semi-arid Mediterranean climate, marked by temperate winter and hot summer. The annual average of rainfall is 385mm. Most of the precipitation has Mediterranean origin coming from disturbances from the N and NE. The rain is characterized by irregularity and brutality aggravating the effect action on the ground not protected by the vegetal cover. The temperature is influenced by the proximity of the Mediterranean coast which reduces the thermal amplitude, the minimum average of winter, being mild, reaches 10 degrees, while the maximum average of summer is moderate, it reaches 29 degrees.

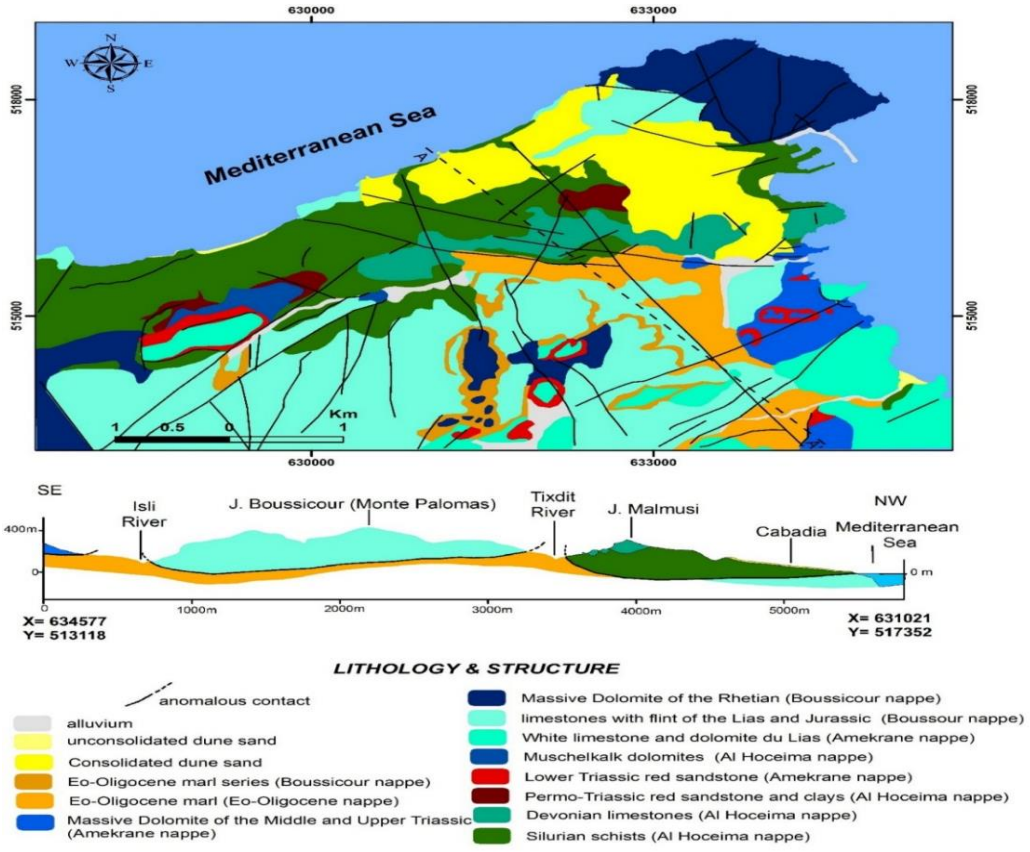

Figure 2: map and geological section showing the lithology and structure of the Bokkoya massif in Al Hoceima region (Geological Map of Al Hoceima, scale 1/50000)

MATERIALS AND METHODS

Figure 3 shows the methodological approach adopted for the analysis of landslide susceptibility in Al Hoceima city based on weight of evidence. This approach consists of five steps:

1) Acquisition and preparation of data to be integrated for landslide susceptibility modeling.
2) Calculation of the weighted values of the causative factors.
3) Assessment of the conditional independence of causal factors from landslides.then, the construction of neo-predictive variables.
4) Probabilistic modelling of landslides based on evidence theory.
5) Validating the results obtained and choosing the best model.

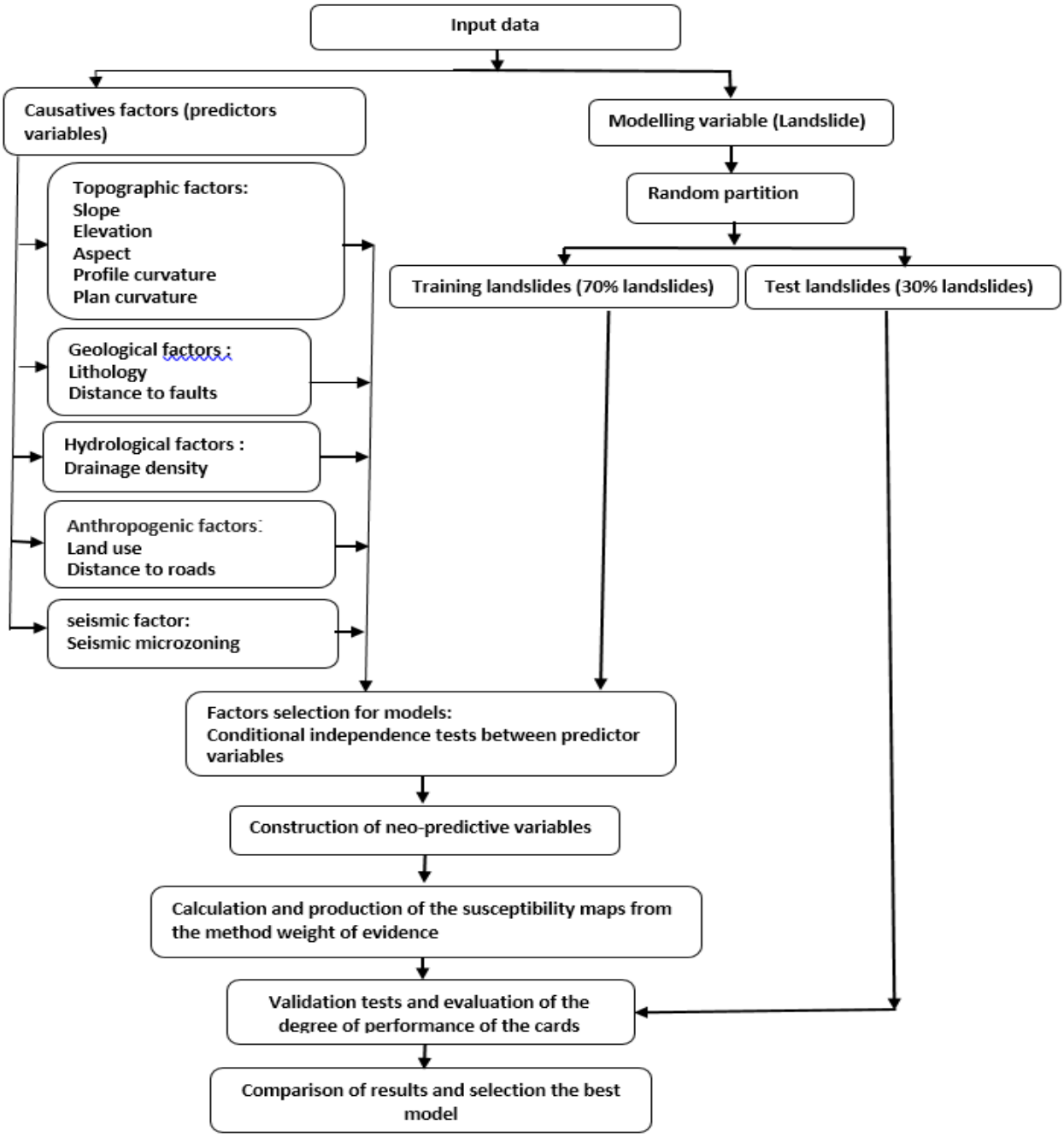

Figure 3: Flowchart showing the data source and the considered steps to produce the landslide susceptibility map

Description of the "weight of evidence" model:

The study aims to assess the susceptibility to landslides using the weight of evidence model. This method has been applied in several fields, initially in medicine (Ezzine et al., 2008; Spiegelhater and Kill-Jones, 1984), then in geology in the field of mineral exploration (Bonham-Carter, 1994); but recently, this method has been used in many studies for the risk assessment of landslide risk (Van Westen, 1993 ; Corominas et al., 2014 ; Thiery, 2007; Ezzine et al., 2008; Mastere, 2011).

This method is based on the assumption that future events will occur under conditions similar to those in the past (Thiery 2007). This approach considers the landslide phenomenon as a variable to be modelled (S) and the causative factors that cause the triggering conditions or the reactivation of this phenomenon as predictive variables (B) (Ezzine et al., 2008 ; Thiery, 2007 ; Mastere, 2011). It takes into consideration data from historical events to calculate the weights of each predictor variable contributing to the occurrence of landslides.

A detailed description of the mathematical formulation of the method is given below:

The probability of occurrence of the phenomenon (S), according to the weight of evidence model, is based on a log-linear version of Bayes general theorem and on the concepts of a priori probability and a posteriori probability (Van Westen, 1993 ; Bonham-Carter, 1994). The a priori probability is determined by the occurrence of a landslide in the A_T (Total Studied Area) zone, without taking into account the causative factors of these phenomena, it is simply the density of landslides in the study area.

$$P(S)=\frac{A_s}{A_T} \qquad (1)$$

The next step is to examine the relationship between the occurrence of a landslide event and the presence of a condition or evidence of a causative factor. Figure 4 shows this relationship between the variable to be modelled and the predictive variable, it can be expressed by the following conditional probabilities:

$$P\{S/B\} = \frac{P\{S \cap B\}}{P\{B\}} \qquad (2)$$

$$P\{S/\bar{B}\} = \frac{P\{S \cap \bar{B}\}}{P\{\bar{B}\}} \qquad (3)$$

Using the conditional probability formula, the last equations can be written as follow:

$$P\{S/B\} = P\{S\}\frac{P\{B/S\}}{P\{B\}} \qquad (4)$$

$$P\{S/\bar{B}\} = P\{S\}\frac{P\{\bar{B}/S\}}{P\{\bar{B}\}} \qquad (5)$$

Bonham-Carter (1994) defined two weights for each predictor variable, a negative weight (W^-)and a positive one (W^+), their values depend on the relationship between past landslide events and predictive variables. These weights are calculated according to the probability “odds” or “logit” which is defined as follow:

$$Odds = \frac{Probability\ that\ the\ event\ will\ occur}{Probability\ that\ the\ event\ will\ not\ occur} = \frac{P}{1-P} \qquad (6)$$

Where P is the a posteriori probability of an event occurring

$$O\{S|B\} = O\{S\}.\frac{P\{B|S\}}{P\{B|\bar{S}\}} \qquad (7)$$

$$O\{S|\bar{B}\} = O\{S\}.\frac{P\{\bar{B}|S\}}{P\{\bar{B}|\bar{S}\}} \qquad (8)$$

$$\ln O\{S|B\} = \ln O\{S\} + \ln\frac{P\{B|S\}}{P\{B|\bar{S}\}}$$

$$\text{logit}\{S|B\} = \text{logit}\{S\} + w^{+} \qquad (19)$$

$$\ln O\{S|\bar{B}\} = \ln O\{S\} + \ln\frac{P\{\bar{B}|S\}}{P\{\bar{B}|\bar{S}\}}$$

$$logit\{S|\bar{B}\} = \text{logit}\{S\} + w^{-} \qquad (10)$$

$$W^{+} = \ln\frac{P\{B|S\}}{P\{B|\bar{S}\}} \qquad (11)$$

$$W^{-} = \ln\frac{P\{\bar{B}|S\}}{P\{\bar{B}|\bar{S}\}} \qquad (12)$$

The contrast value C can be used as a guide to determine the relative weight of each predictor variable. In addition, it provides information on the association between these variables and the occurrence of landslide phenomena, it is defined as follow:

$$C = W^{+} - W^{-} \qquad (13)$$

If C is positive, it indicates a positive correlation between the predictor variable and the variable to be modeled. C is negative shows a negative correlation between the two, and C equal to 0 indicates that the distribution is spatially independent (Ezzine, 2008).

Concerning the cartography of landslide susceptibility or probability, this phenomenon may be associated with one or more predictive variables. Therefore, it is necessary to combine the positive weights of all these variables, but provided that they are conditionally independent of each other. Areas with a high weight correspond to a higher probability of finding (S). The general expression for combining n factors is given by the following equation (Bonham-Carter, 1994):

$$logit\{S|B_1^k \cap B_2^k \cap B_3^k \ldots\ldots \cap B_n^k\} = logit\{S\} + \sum_{i=1}^{n} W_i^{+} \qquad (14)$$

Conditional Independence Test:

The application of weight of evidence model assumes that the predictive variables are independent of each other in relation to the variable to be modeled (landslide) inventoried and included in the analysis (Thiery et al., 2004). It is therefore necessary to test the conditional independence between all predictor variables before integrating them to create the landslide probability or susceptibility map.

To test the conditional independence between two predictor variables, we used the following equation:

$$N\{B_1 \cap B_2 \cap S\} = \frac{N\{B_1 \cap S\}\, N\{B_2 \cap S\}}{N\{S\}} \qquad (15)$$

The left side of equation (15) is the number of landslide events observed in the area of overlap of two predictor variables B1 and B2. The right side is the predicted number of landslides occurrence in this overlap area. This relationship is presented in a contingency table to test the conditional independence between these two variables (Table 1). Next, the chi-square test ($\mathcal{X}^2$) was applied to all pairs of predictor variables to evaluate the variation between expected (Ei) and observed (Oi) landslide frequencies using equation (16).

$$\mathcal{X}^2 = \sum_{i=1}^{n} \frac{(O_i - E_i)^2}{E_i} \qquad (16)$$

		Variable B1		
		Absence	Presence	Total
Variable B2	Absence	$O_1 = \{\overline{B_1} \cap \overline{B_2} \cap S\}$ $(E_1 = \{\overline{B_1} \cap S\} * \{\overline{B_2} \cap S\}/\{S\})$	$O_3 = \{B_1 \cap \overline{B_2} \cap S\}$ $(E_3 = \{B_1 \cap S\} * \{\overline{B_2} \cap S\}/\{S\})$	$\{\overline{B_2} \cap S\}$
	Presence	$O_2 = \{\overline{B_1} \cap B_2 \cap S\}$ $(E_2 = \{\overline{B_1} \cap S\} * \{B_1 \cap S\}/\{S\})$	$O_4 = \{B_1 \cap B_2 \cap S\}$ $(E_4 = \{B_1 \cap S\} * \{B_2 \cap S\}/\{S\})$	$\{B_2 \cap S\}$
	Total	$\{\overline{B_1} \cap S\}$	$\{B_1 \cap S\}$	$\{S\}$

Table I: Contingency table for testing conditional independence.

Then, the comparison between actual and theoretical Chi-square values ($\mathcal{X}^2$) for each pair of predictor variables and for the variable to be modeled, according to 1 degree of freedom and at the 99% confidence level ($\mathcal{X}^2$= 6.64) had to be determined (Dai & Lee, 2002). Above this value, $\mathcal{X}^2$indicates the presence of a conditional dependence between the two variables. In this case, the two variables cannot be integrated in the modeling process. Nevertheless, it is recommended to combine them to create a neo-predictive variable (van Westen, 1993; Thiery et al., 2007; Bonham-Carter, 1991; Mastere, 2011).

Validation of results:

The validation of the results obtained by the model is represented graphically, using the ROC (Receiver Operating Characteristic) curve. This curve is a statistical tool that allows us to assess the performance of the landslide susceptibility model by comparing the validity of forecasts of landslide phenomena of other events observed in the field. In this analysis, the construction of the ROC curve is carried out using data from landslides reserved for validation (30% of the set of landslides observed in the field) and which were not included in the data used to create the susceptibility map. This representation mode is based on the threshold values which separate stable and unstable terrains. This curve shows the "Specificity" on the abscissa and the "Sensitivity" on the ordinate. "Sensitivity" or (True Positive Rate) represents the proportion of pixels affected by landslides correctly classified as unstable. The "Specificity" or (1- False Positive Rate) represents the proportion of pixels not affected by landslides correctly classified as stable (Fressard, 2013). The calculation of the sensitivity and the specificity associated with the different threshold values is expressed by the following formulas (Devkota et al., 2013;Thiery, 2007):

$$\text{Sensitivity} = \frac{\text{TP}}{\text{TP} + \text{FN}} \qquad (17)$$

$$\text{Specificity} = 1 - \text{False Positive Rate} = 1 - \frac{\text{FP}}{\text{FP} + \text{TN}} \qquad (18)$$

TP: True Positive, TN: True Negative; FP: False Positive; FN: False Negative;

The area under the curve of ROC or AUC (Area Under Curve) can be used as a measure to assess the discriminating power of the model. The more the area under the curve is larger, the more the capacity of the model's ability to predict the presence and absence of landslides is better (Dumlao & Victor, 2015). AUC is calculated by adding the areas of the polygons between the different threshold values (Vakhshoori & Zare, 2016):

$$AUC = \sum_{i=1}^{n+1} \frac{\sqrt{(x_i - x_{i+1})^2} * (y_i + y_{i+1})}{2} \qquad (19)$$

Where x_i is the specificity and y_i is the sensitivity to the threshold i.

Preparation and construction of a database of factors related to the occurrence of landslides:

Landslides have been already mapped for the entire city of Al Hoceima. These events are represented by polygons based on the inventory of landslides and the interpretation of Google Earth satellite images as well as on mobile GPS mapping (MobileMapper) to locate landslides and determine its limits. These have been demarcated as landslide areas, but in some areas where there are signs of ground instability such as tension cracks or tilted trees, these areas have been included in the mapping. In this analysis, the total number of the landslides inventoried forming rotational and translational movements was divided into two distinct sets: 70% of older landslides (106 events) are used to build the model of landslide sensitivity and 30% (45 events) of landslides recently reactivated or triggered are used to validate this model (Figure 4 and 5) (Bui et al., 2011; Ozdemir & Altural, 2013;Vakhshoori & Zare, 2016). The last together, independent of the model, can be seen as "future" landslides which may explain how model and causal factors predict future landslides.

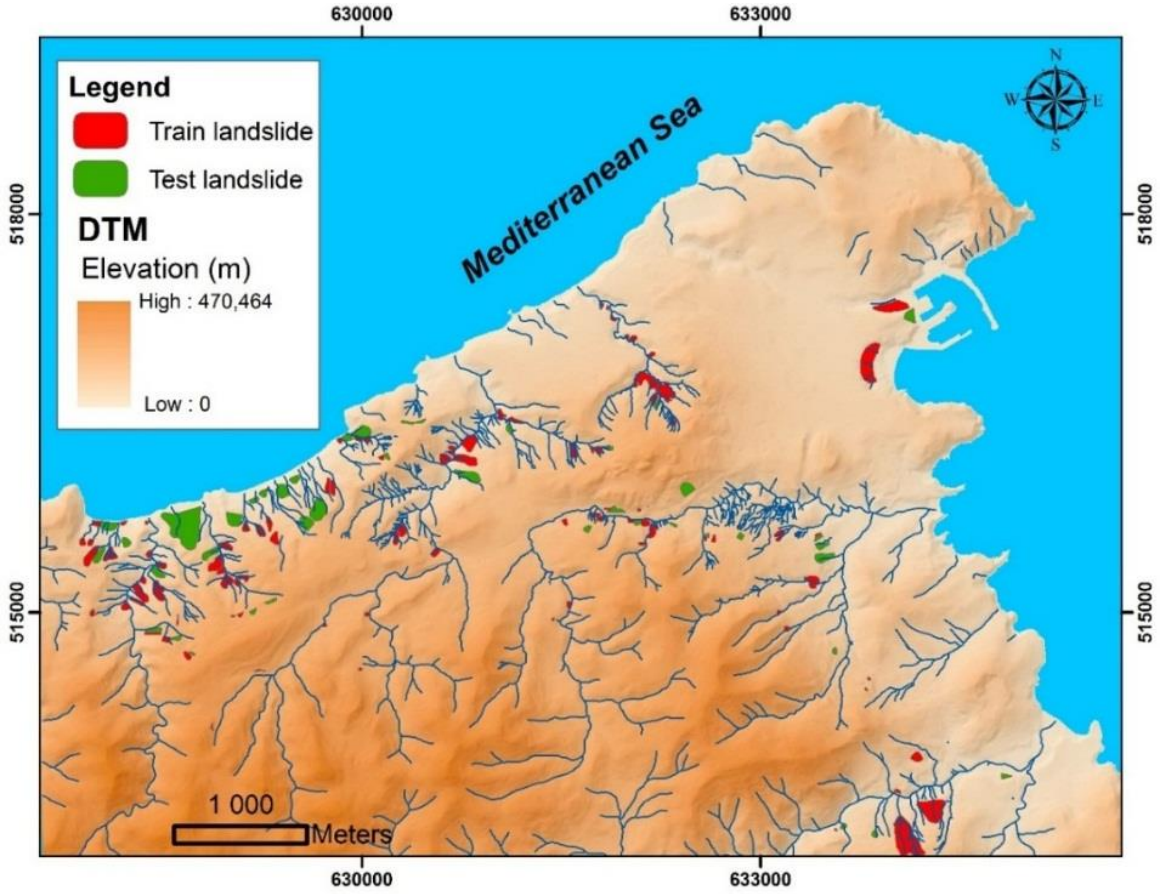

Figure 4: Landslide inventory map showing two sets of landslides used in susceptibility analysis

Photo 1 : Rotational landslide affects Eo-oligocene marls in the Boujibar district.

Photo 2: Complex landslide characterized by numerous escarpments affecting the marl soils in the Boujibar district.

Photo 3 : Escarpment of a rotational slide affects the schistous terrains in the Talayoussef sector

Photo 4 : Translational landslide affects the schist soils beside the Chafarina Hotel located in Talayoussef

Figure 5: Representative photos of some inventoried landslides in the city of Al Hoceima

The basis of the primary acquisition of spatial data is represented by the restitution plan of the city of Al Hoceima on a 1/2000 scale (2016 edition). A digital Terrain Model (DTM) was generated from data for contour lines traced in this plane (equidistance of 1m). It is offered at a resolution of 5m and projected according to the Moroccan projection system Lambert zone 1 (Merchich / North Morocco). It serves in mapping thematic layers of certain morphological parameters: slope, elevation, aspect, profile curvature, and plan curvature. From the image of Google Earth at high spatial resolution (2016 edition), we obtained the thematic layers of the land use: the different categories of land use and distance to roads. The density of the hydrographic network was produced from the river streams drawn on the plan restitution using the Spatial Analyst Tools "Line density" command. Geological factors are considered to be the most influential factors in the landslide susceptibility mapping due to their influence on the mechanical and structural characteristics of lithological units. In this study, the lithology and faults are extracted from the Al Hoceima geological map at 1/50000 (1984 edition). Finally, to evaluate the seismic factor in this analysis, we used the 1/40000 scale seismic microzonation map produced by Talhaoui et al. (2004). Although, the precipitation factor is considered to be relatively uniform due to a single station that covers the entire territory of Al Hoceima and was therefore not included in the analysis. The diversity of the sources of these data is a bit varied in their scales, which affects the precision of the susceptibility model. To avoid this problem, all the thematic layers were integrated into a geographic information system (GIS) and are subject to georeferenced management, then all thematic layers have been converted to a raster format (Figure 6). The mesh size of all the causal factor maps used in this analysis was fixed at 5 * 5. This dimension is the same size as a DTM developed for this study.

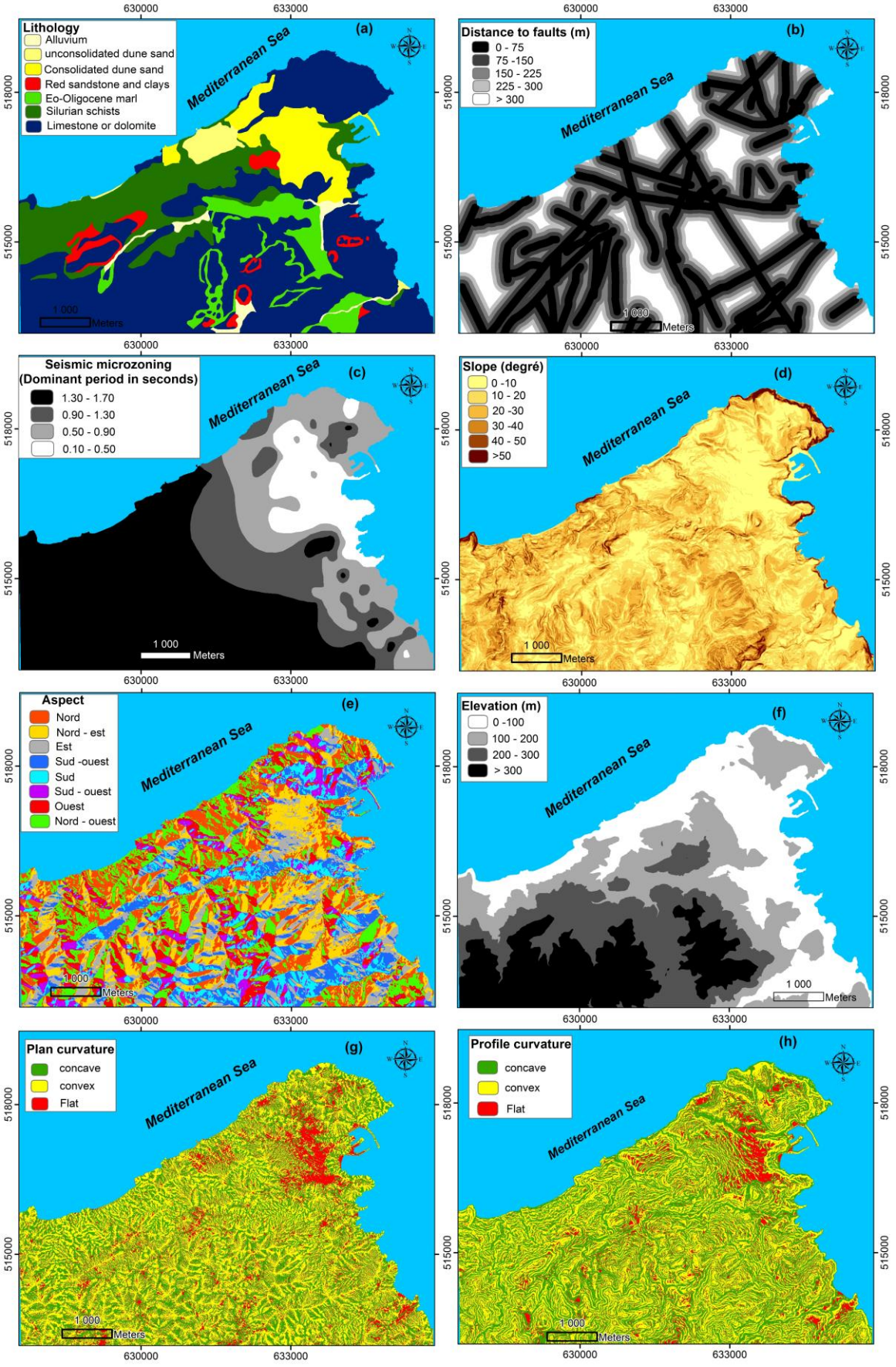
630000
633000
518000
515000
(a)
Lithology
Alluvium
unconsolidated dune sand
Consolidated dune sand
Red sandstone and clays
Eo-Oligocene marl
Silurian schists
Limestone or dolomite
Mediterranean Sea
1 000
Meters
(b)
Distance to faults (m)
0 - 75
75 -150
150 - 225
225 - 300
> 300
(c)
Seismic microzoning
(Dominant period in seconds)
1.30 - 1.70
0.90 - 1.30
0.50 - 0.90
0.10 - 0.50
(d)
Slope (degré)
0 -10
10 - 20
20 -30
30 -40
40 - 50
>50
(e)
Aspect
Nord
Nord - est
Est
Sud -ouest
Sud
Sud - ouest
Ouest
Nord - ouest
(f)
Elevation (m)
0 -100
100 - 200
200 - 300
> 300
(g)
Plan curvature
concave
convex
Flat
(h)
Profile curvature
concave
convex
Flat

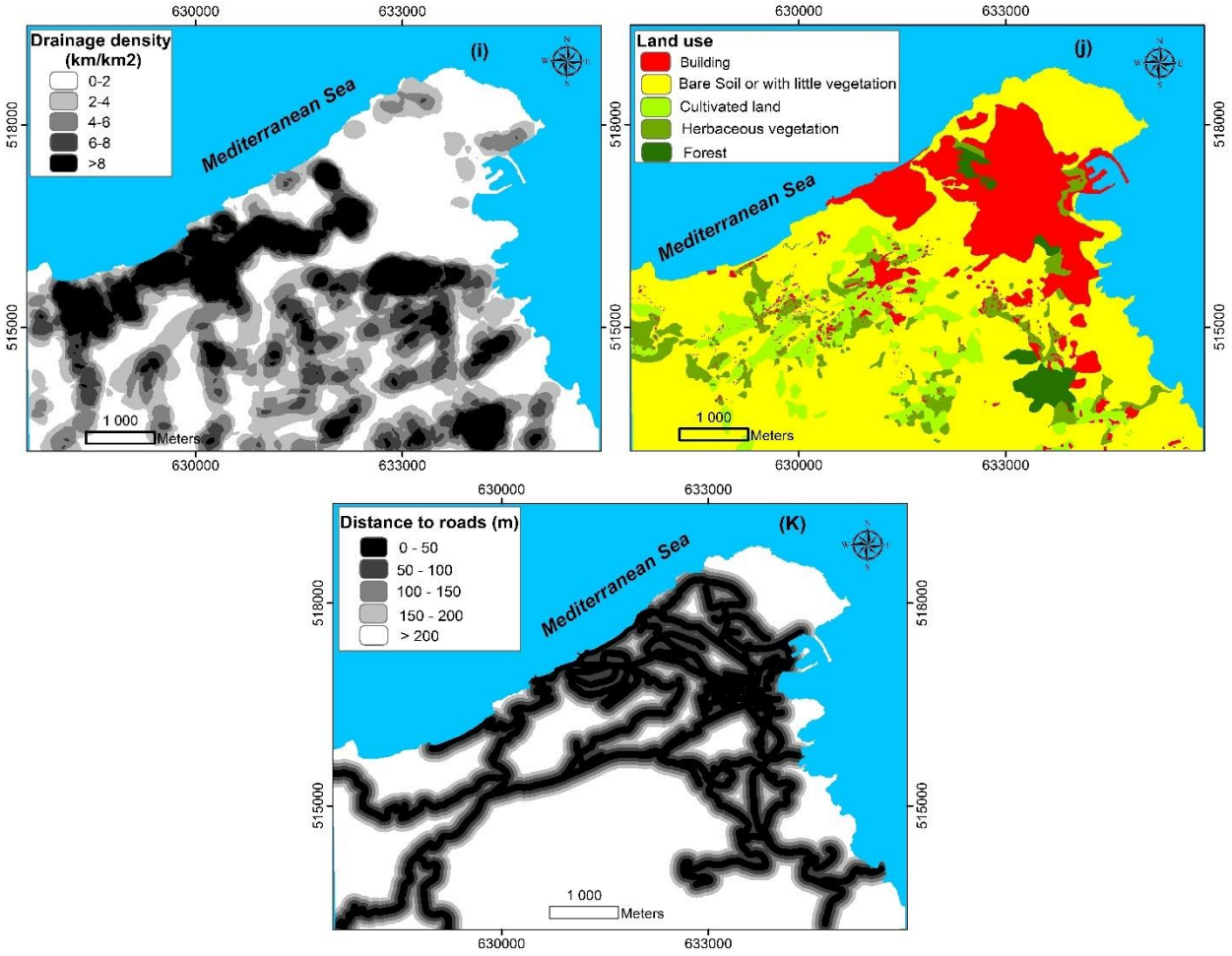

Figure 6. landslides causal factors: a) lithology, b) distance to faults, c) seismic microzoning, d) slope, e) aspect, f) Elevation, g) plan curvature, h) profile curvature, i) drainage density, (j) land use, k) distance to roads.

RESULTS

Calculation and interpretation of weighted values:

The application of weight of the evidence approach method has been carried out following the steps summarized in the previous paragraphs. Table 2 shows the results of the calculation of the weighting values obtained for eleven factors: lithology, slope, distance to faults, density of the hydrographic network, slope exposure, land use, seismic microzoning, hypsometry, transverse curvature, longitudinal curvature and distance to roads.

The relationship between landslides and causative factors is as follows:

In the case of the slope, the higher the slope, the greater the occurrence of landslides. For example, below 20%, the contrast is very low, reaching -2.141, and above 20% up to 50%, the contrast is greater than 0.58. This indicates that the occurrence of landslides increases with the slope.

In the case of the geological factors, such as lithology and faults: Lithology has shown a very strong effect on landslides. The positive contrast value was noted in areas which are very sensitive to landslides (C=2.03 for Silurian shales, C= 1.50 for Eo-oligocene marls and C= 1.086 for Triassic red sandstones and argillites). Most

landslides occur mainly along faults. The contrast value is positive at a distance less than 150m from the fault (C> 0.22), indicating a favorable area for landslides, whereas at a distance greater than this value, the contrast becomes negative, indicating an unfavorable area for landslides.

The values obtained by the analysis of the drainage factor show that the areas affected by landslides are characterized by a very high density of the river network (> 8km/km2 or 80m/Ha). This can be attributed to the fact that the landslide can be caused by gullying or by high density of the river drainage

In the case of profile and plane curvatures, the contrast value is positive in the concave morphology (C= 0.429 and C= 0.252, respectively), on the other hand, it is negative in the convex morphology and in the plane areas. The reason is that the concave morphology retains rainwater longer and favors the occurrence of landslides.

In the case of slope exposure, landslides are very abundant on the north (C= 0.930), northeast (C= 0.208) and northwest (C= 0.220) slopes. This is due to the influence of disturbances of Mediterranean origin. These slopes constitute barriers that intercept these disturbances, which can generate stormy rainfall and therefore amplify the triggering or reactivation of landslides. On the other hand, the frequency of landslides is very low in the other slopes that are sheltered from these disturbances. This is explained by negative contrast values.

In the case of land use, the highest contrast values are found in areas of bare soil or with some vegetation (C= 0.63) and in areas of tree or shrub or herbaceous vegetation (C= 0.471).

For seismic microzoning, the contrast is very high in the interval (1.30- 1.70). This is an area of ancient landslides with strong fractures and steep slopes, characterized by deposits with loose and unconsolidated structure. These conditions are the main disturbing elements of the slope equilibrium in the face of seismic events.

In the case of altitude, the contrast value is positive at altitudes below 200m (C>0.88). While it is negative at altitudes above 200m. This may be due to the dominance of a landslide sensitive lithology and a very high drainage density, which favors a high possibility of landslide occurrence.

In the case of the distance to roads, the contrast is positive at a distance greater than 100m. This means that the number of landslides located in the vicinity of roads is relatively small compared to the number of the other landslides in area of study. This indicates that there are other factors involved in the occurrence of these phenomena.

Causative factor (predictor variable)	**Total pixels of each class**	**landslide pixels in each class**	**W+**	**W-**	**C**
Distance to faults (m)					
0-75	397524	5583	0.147	-0.080	0.228
75-150	300746	4392	0.187	-0.070	0.257
150-225	201797	2445	-0.002	0.000	-0.003
225-300	128301	1488	-0.047	0.005	-0.052
300>	184309	818	-1.014	0.109	-1.123
Aspect					
North	223551	5314	0.684	-0.247	0.930

Northeast	188615	2716	0.173	-0.035	0.208
East	158663	1094	-0.571	0.064	-0.635
Southeast	132108	835	-0.659	0.058	-0.717
South	107835	451	-1.074	0.063	-1.137
Southwest	84852	332	-1.141	0.050	-1.191
West	122311	1164	-0.246	0.024	-0.271
Northwest	194100	2820	0.182	-0.039	0.220
Flat	642	0		0.001	
Elevation (m)					
0-100	368813	7527	0.528	-0.357	0.884
100-200	311388	6676	0.578	-0.310	0.888
200-300	259872	503	-1.847	0.209	-2.056
>300	272604	20	-5.121	0.257	-5.378
Drainage density (km/km^2)					
0-2	444850	767	-1.963	0.410	-2.372
2-4	254135	1354	-0.831	0.141	-0.971
4-6	202485	723	-1.233	0.134	-1.367
6-8	135173	1361	-0.189	0.021	-0.211
>8	176034	10521	1.643	-1.105	2.748
Lithology					
Limestone or dolomite	713233	247	-3.569	0.887	-4.456
Silurian schists	216223	9044	1.267	-0.762	2.030
Eo-Oligocene marl	101143	4168	1.252	-0.248	1.500
Red sandstone and clays	28906	973	1.042	-0.045	1.086
Consolidated dune sand	104548	197	-1.874	0.078	-1.951
unconsolidated dune sand	26346	81	-1.383	0.017	-1.399
Alluvium	22278	16	-2.839	0.018	-2.857
Seismic microzonation (dominant periods)					
0.10s- 0.50s	123850	1362	-0.100	0.011	-0.111
0.50s- 0.90s	226727	2000	-0.323	0.062	-0.385
0.90s- 1.30s	214488	1905	-0.316	0.057	-0.373
1.30s - 1.70s	647612	9459	0.187	-0.267	0.455
Land use					
Building	215858	348	-2.030	0.174	-2.204
Herbaceous vegetation	92886	1716	0.426	-0.045	0.471
Cultivated land	110238	1445	0.077	-0.008	0.085
Bare Soil or with little vegetation	766033	11217	0.190	-0.440	0.629
Forest	27662	0		0.023	
Slope (degree)					
0°-10°	287072	525	-1.904	0.237	-2.141
10°-20°	406521	3950	-0.225	0.097	-0.323
20°-30°	352762	6230	0.380	-0.209	0.589
30°-40°	128107	3448	0.811	-0.157	0.968
40°-50°	24843	571	0.649	-0.019	0.668

>50°	13372	2	-4.409	0.011	-4.420
Plan curvature					
Concave	474926	7301	0.239	-0.190	0.429
Flat	181680	1147	-0.660	0.082	-0.742
convexe	556071	6278	-0.074	0.059	-0.132
Profile curvature					
Concave	526951	7308	0.135	-0.117	0.252
Flat	144874	899	-0.677	0.065	-0.742
Convexe	540852	6519	-0.008	0.006	-0.014
Distance to roads (m)					
0-50	256957	2272	2.053	0.071	-0.084
50-100	167548	2217	1.878	-0.015	-0.044
100-150	118957	1569	1.880	-0.010	0.010
150-200	93084	1506	1.791	-0.028	0.035
>200	576131	7162	1.905	-0.022	0.079

Table 2: Spatial correlation between each causative factor and landslides. W+ : Positive weight ; W─ : Negative weight ; C : Contrast

Evaluation of conditional independence:

Before proceeding with the calculation of the probability of landslides occurrence, a chi-square test ($\mathcal{X}^2$) was calculated to assess the conditional independence between the predictor variables. This calculation was performed taking into account that one pixel representing the barycentre of each landslide (Thiery et al., 2004). In this step, all the predictor variables used in this analysis were converted into a binary configuration (presence or absence of landslides) based on the positive and negative weights calculated for each variable (Mezughi et al., 2011; Pradhan & Buchroithner, 2010; Regmi et al., 2010). The classes of the factors which have positive weights have been assigned as factors for the presence of a landslide event, and classes which have negative weights are considered to be factors for the absence of a landslide event.

The reading of table 3 allows us to identify the test of independence between all pairs of binary predictive variables. The chi-square value ($\mathcal{X}^2$) calculated for each pair is compared to the table value for 1 degree of freedom at the 99% confidence level (6.64). The comparison of the theoretical $\mathcal{X}2$ and the observed $\mathcal{X}2$ shows that 6 pairs of variables present a conditional dependence. This is the case of the factor "altitude" with the factors "drainage density", "lithology" and "seismic microzoning", it is also the case of transverse curvature with the slope and longitudinal curvature, as it is the case of the density of the hydrographic network with the distance to roads. These pairs of factors cannot be integrated into the modelling process. However, they can be combined in a new predictive variable (neo-predictive variable) and then introduced into the spatial analysis as a single variable (Van Westen, 1993 ; Bonham-Carter, 1994 ; Ezzine et al., 2008; Mastere, 2011; Thiery, 2007). In my case, the combination of river network density and road distances and between transverse and longitudinal curvature, is not possible, because they are conditionally dependent. Given that these variables are among the most important factors in triggering landslides in Al Hoceima, I propose to introduce them in the spatial analysis as a neo-predictive variable "density of the hydrographic network + distance to roads". Thus, the grouping of classes of these neo-predictive variables was done as follows:

a) - Density of the hydrographic network + distance to roads (NV(DD+DR)): were considered to be the most important factors influencing the occurrence of landslides. They generally represent the area most threatened by slope instability. Thus, five classes are considered:

- Class 1 : density from 0 to 2 km/km2 + distance to the road greater than 200 m
- Class 2 : density of 2 to 4 km/km2 + distance to the road between 150 and 200 m
- Class 3 : density of 4 to 6 km/km2 + distance to the road between 100 and 150 m
- Class 4 : density of 6 to 8 km/km2 + distance to the road between 50 and100 m
- Class 5 : density greater than 8 km/km2 + distance to the road less than 50 m

b) - transverse curvature + longitudinal curvature (NV(PC+PT)): can be easily grouped together from a geomorphological point of view. They depend mainly on the concavity and convexity of the surface. These geomorphological characteristics can lead to a change in the whole slope and often promote instability in slopes that are in potential equilibrium. Thus, the grouping "transverse curvature + longitudinal curvature" includes the three classes:

- Class 1 : longitudinal curvature (concave form) + transverse curvature (concave shape)
- Class 2 : longitudinal curvature (flat form) + transverse curvature (flat form)
- Class 3 : longitudinal curvature (convex form) + transverse curvature (convex form)

The variables to be combined have been tested by Cramer's V test (Thiery, 2007; Mastere, 2011)in order to explore the level of association between them, as recommended. The value obtained of the Cramer's V is equal to 0.29 for (NV(DD+DR)) and 0.37 for (NV(PC+PT)). These values indicate a medium to strong relationship between the combined factors (Kim, 2017), indicating that we can then group these variables together and introduce them into this analysis.

	A	E	DD	L	LU	S	PC	PT	DF	DR	SM
A		1.034	0.654	5.090	0.193	0.592	1.875	0.158	0.911	0.863	1.976
E			**8.321**	**7.128**	2.195	0.027	3.99	0.596	3.317	5.653	**7.847**
DD				1.210	5.936	2.736	1.497	2.194	0.361	**9.299**	0.110
L					0.599	0.027	2.023	0.596	3.317	2.927	3.447
LU						0.149	0.159	0.214	2.630	0.113	0.824
S							0.399	**7.323**	0.019	2.604	1.275
PC								**14.75**	0.067	5.164	0.281
PT									0.030	0.011	0.581
DF										0.318	4.962
DR											1.023
SM											

Table 3: Conditional Independence Assessment Results. A: Aspect, E: Elevation, DD: Drainage density, L: Lithology, LU: Land use, S: Slope, PC: Profile curvature, PT: Plan curvature, DF: Distance to faults, DR: Distance to roads, SM: Seismic microzoning. Values in bold indicate a conditional dependence between two factors. The chi-square test is performed with 1 degree of freedom and at a confidence level of 99% ($\mathcal{X}2$= 6.64).

Combination of the factor maps and model validity:

To examine the influence of each factor on the predictive power of our hazard map, we selected eight combinations of different independent factors (Table 4) (Mezughi et al., 2011; Pradhan et al. 2010; Thiery et al. 2004; Mastere, 2011), representing topographic, hydrological, geological, seismic and land use factors (Regmi et al., 2010; Mezughi et al., 2011). Then, the final probability for each mesh and for each model (or combination) is calculated using the a posteriori probability equation (14) (Bonham-Carter, 1994; Chamorro, 2010). This allows mapping of twelve landslide susceptibility maps in Al Hoceima (Figure 7).

Model	Combination of factors	AUC
1	M1= S+A+PC+DD+L+DF+LU+SM	0.899
2	M2= S+ DD+ L+DF+LU	0.889
3	M3= EV+ CL+DRH+L+DF+OS+MS	0.891
4	M4= S+A+PC+DD+DF+LU+SM	0.829
5	M5= S+A+PC+DD+LU	0.822
6	M6= S+A+PC+DF+DD+LU	0.824
7	M7= S+A+PC+DF+DR+LU	0.769
8	M8= S+A+PC+NV(DD+DR)+L+DF+LU	0.900
9	M9= S+PC+L+DF+LU+DR	0.894
10	M10=S+L+DF+PT+DD+SM	0.892
11	M11=S+A+NV(DD+DR)+NV(PC+PT)+L+DF+LU+SM	0.902
12	M12=S+NV(PC+PT)+A+DD+L+DF+LU	0.897

Table 4: Combination of Predictor Variables for twelve models

The predictive or discriminating ability of each model is determined by the area under the curve (AUC) (Figure 8). Based on these values, it can be seen that models 1, 8, 11 and 12 provide good results. Thus, they predict more landslides in the high susceptibility area than the other models. On the other hand, there is a decrease in AUC values for the other models. Model 7 represents the smallest value; this is due to the variables of river system density, lithology and seismic microzoning which are not included in the analysis. In addition, the AUC values for Models 4, 5 and 6 are relatively higher than the previous model, where lithology, fault distance and seismic microzoning factors are not used in the analysis. The absence of these factors in these four models contributes to the decrease in their predictive power. Also, we can see that the distribution of probability classes shows a disturbance in our area of study (Figure 7: M4, M5, M6 and M7), which results in sensitive areas to landslide within the carbonate formations of the Bokkoya massif. Also, the elimination of the slope factor in Model 3 and the slope exposure factors and the longitudinal curvature in Model 2 contributes to a decrease in the AUC value when compared with the values of models that include these factors. This indicates that morphological factors have an influence on landslide genesis. In Model 10, the land cover factor has not been introduced; the decrease in the AUC value attests the great importance of this parameter in the study of landslide hazard. The elimination of the factor of the density of the hydrographic network as well as the seismic factor has relatively decreased the AUC value of model 9. However, the integration of the neo-predictive variables "river network density + distance to roads" and "transverse curvature + longitudinal curvature" increases the predictive power of my model ('M8', AUC = 0.90; 'M11', AUC=0.902; 'M12', AUC=0.897). This shows that the neo-variables formed clearly contribute to the improvement of the predictive power of the model, as well as give very clearly improved results compared to other combinations, especially since they result from the integration of important factors in the genesis of landslides in the studied area. Among the 12 representative combinations of the various factor landslide triggers in the study area, there is one high-prediction combination calculated from

the AUC (area under the curve) prediction curve. This is the combination of model 11 with AUC= 0.902. This value was found from the integration of a set of factors contributing to improve the model predictive power, responsible for landslides in the city of Al Hoceima, namely lithology, faults, slope, relief morphology, slope exposure, hydrographic network, seismicity and land use.

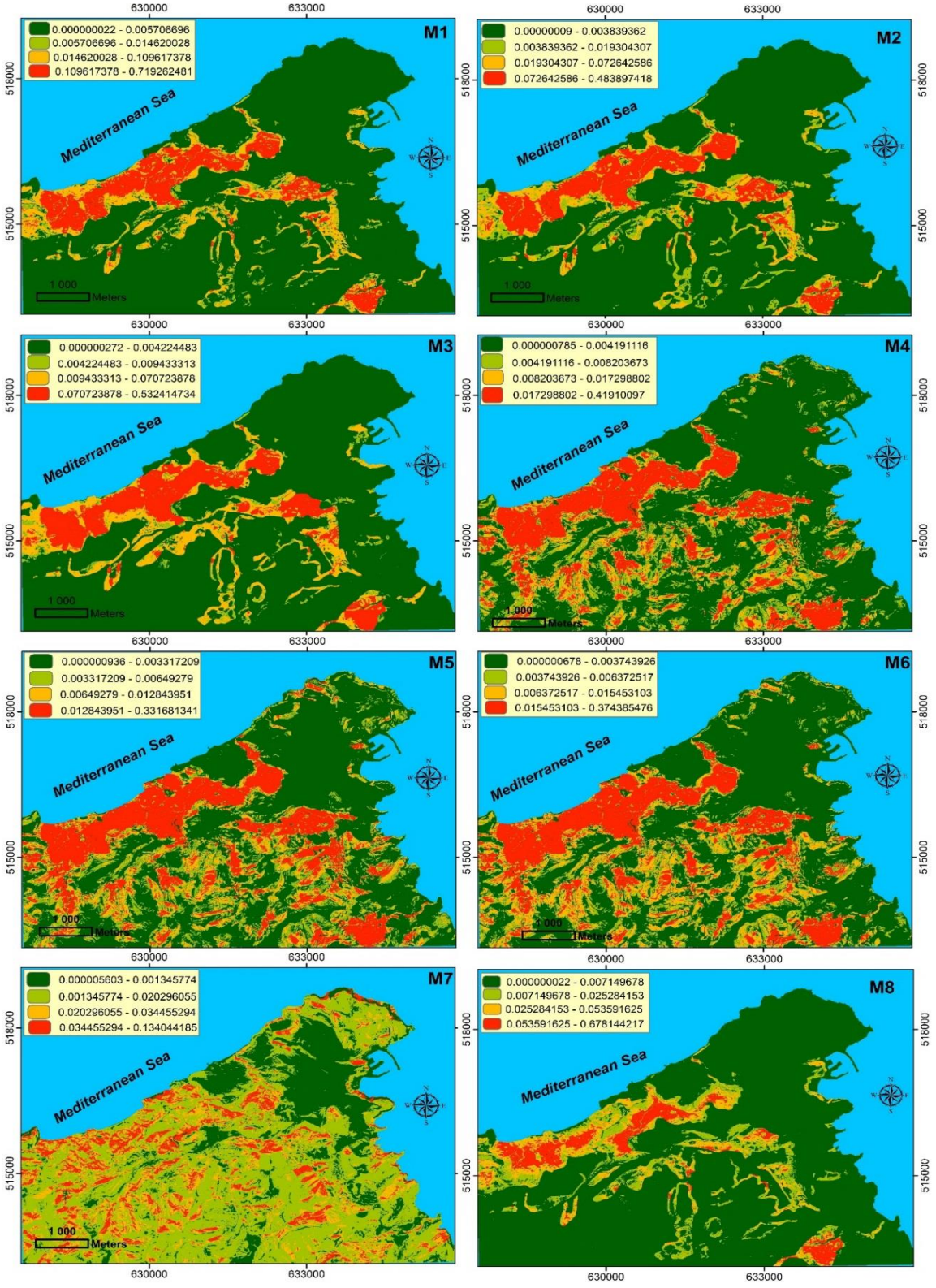

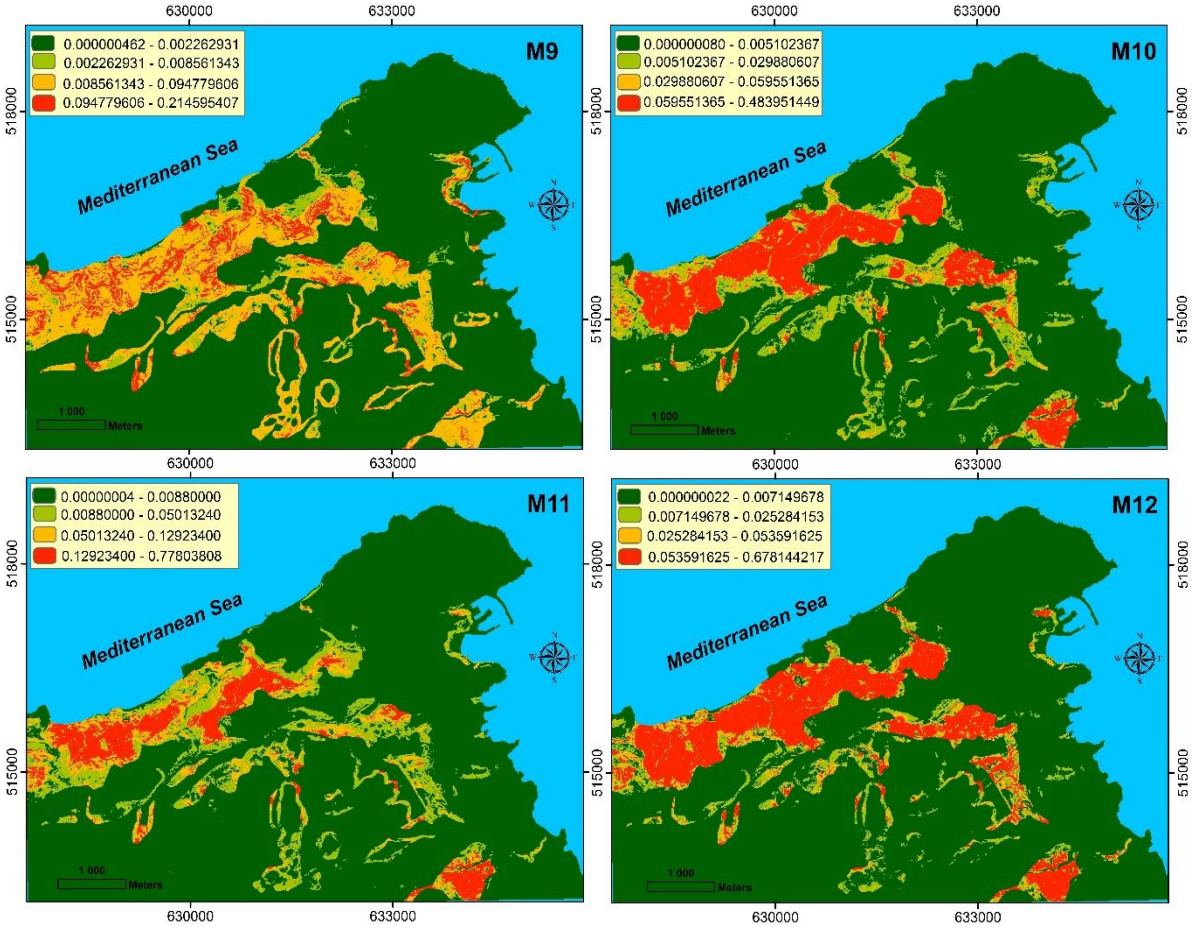

Figure 7: The landslide susceptibility maps of the study area realized from twelve studied combinations.

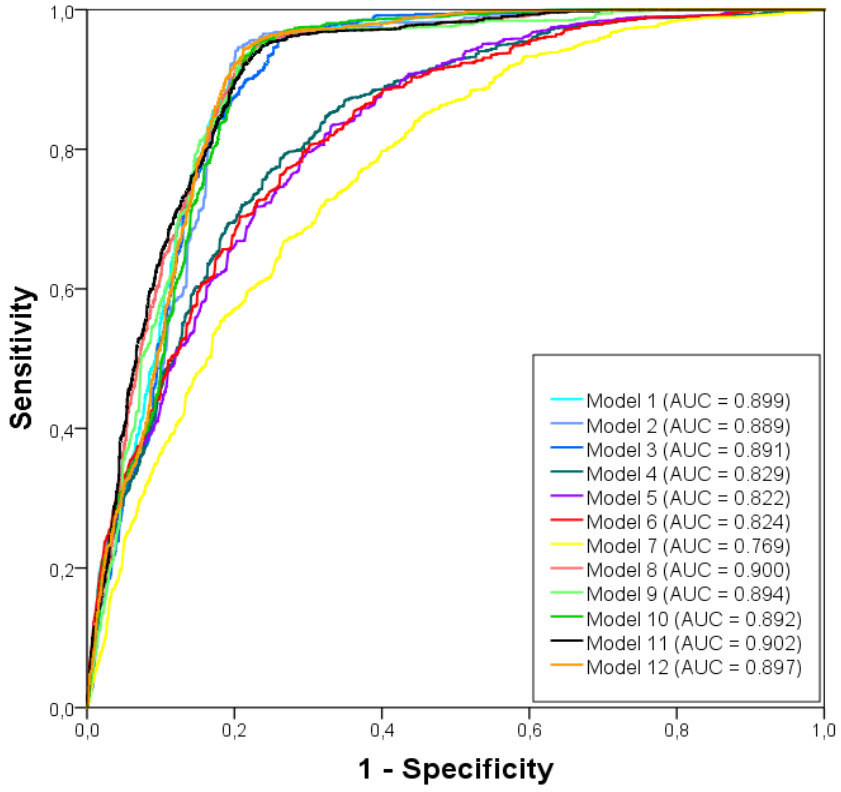

Figure 8: ROC curves obtained by the twelve models studied

Hazard Zoning:

In order to facilitate the reading and interpretation of the hazard map, we have adopted a method frequently used by several authors (Mastere, 2011; Thiery et al., 2004; Van Den Eeckhaut et al., 2009) and from which we will select the classes of hazard landslide. This method reclassifies the map into several intervals based on abrupt changes in the cumulative a posteriori probability curve represented here by thresholds. As in the above cumulative curve (Figure 9), three threshold probabilities have been identified on the curve where the limits of the susceptibility classes have been defined: low (0 – 0.088), moderate (0.088 - 0.05), high (0.05 - 0.129), and very high (0.129 – 0.778). Based on these classes, hazard landslide zoning was carried out in Al Hoceima and its periphery (Figure 10).

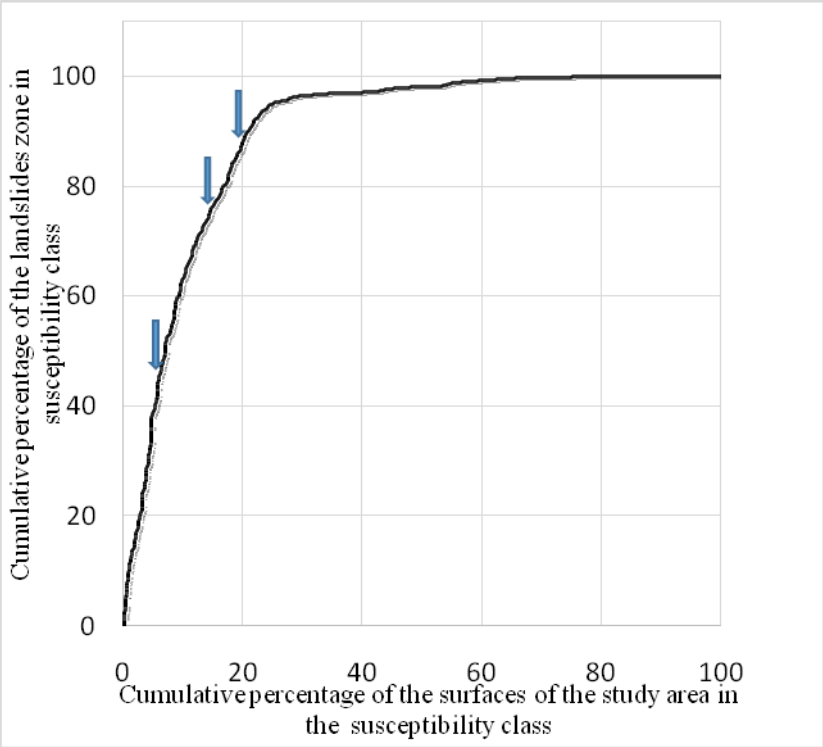

Figure 9: Cumulative probability curve of the landslide hazard. The arrows indicate the thresholds of the different classes of the hazard..

According to this classification, the percentage of surface area of each hazard class was calculated. As shown in Table 5, 78.24% of the area of study is designated as low or no hazardous, with medium hazard areas covering only 10.36% of the area of study. On the other hand, the high and very high hazard zones represent 5.51% and 5.89% respectively. Comparison between the obtained hazard map and the distribution of landslides in the area of study shows that 48.45% of the landslides are located in a very high hazard area, 20.58% fall in a high hazard area, 21.55% fall in a medium hazard area and 9.42% fall in a no or low hazard area.

Table 5: Characteristics of the four classes of susceptibility to landslides

Class	Probability	Susceptibility to landslides	% in study area	% in depletion area
1	0 – 0.0088	Low	78.24	9.42
2	0.0088 - 0.05	Medium	10.36	21.55
3	0.05 - 0.129	High	5.51	20.58
4	0.129 – 0.778	Very High	5.89	48.45

According to this classification, a large part of the area of study is in areas of very low susceptibility. But some central parts of Al Hoceima, in the Bokkoya massif, show some areas of medium susceptibility. The high and very high sensitivity zones are mainly located in the north of the city within the ancient landslides of great magnitude.

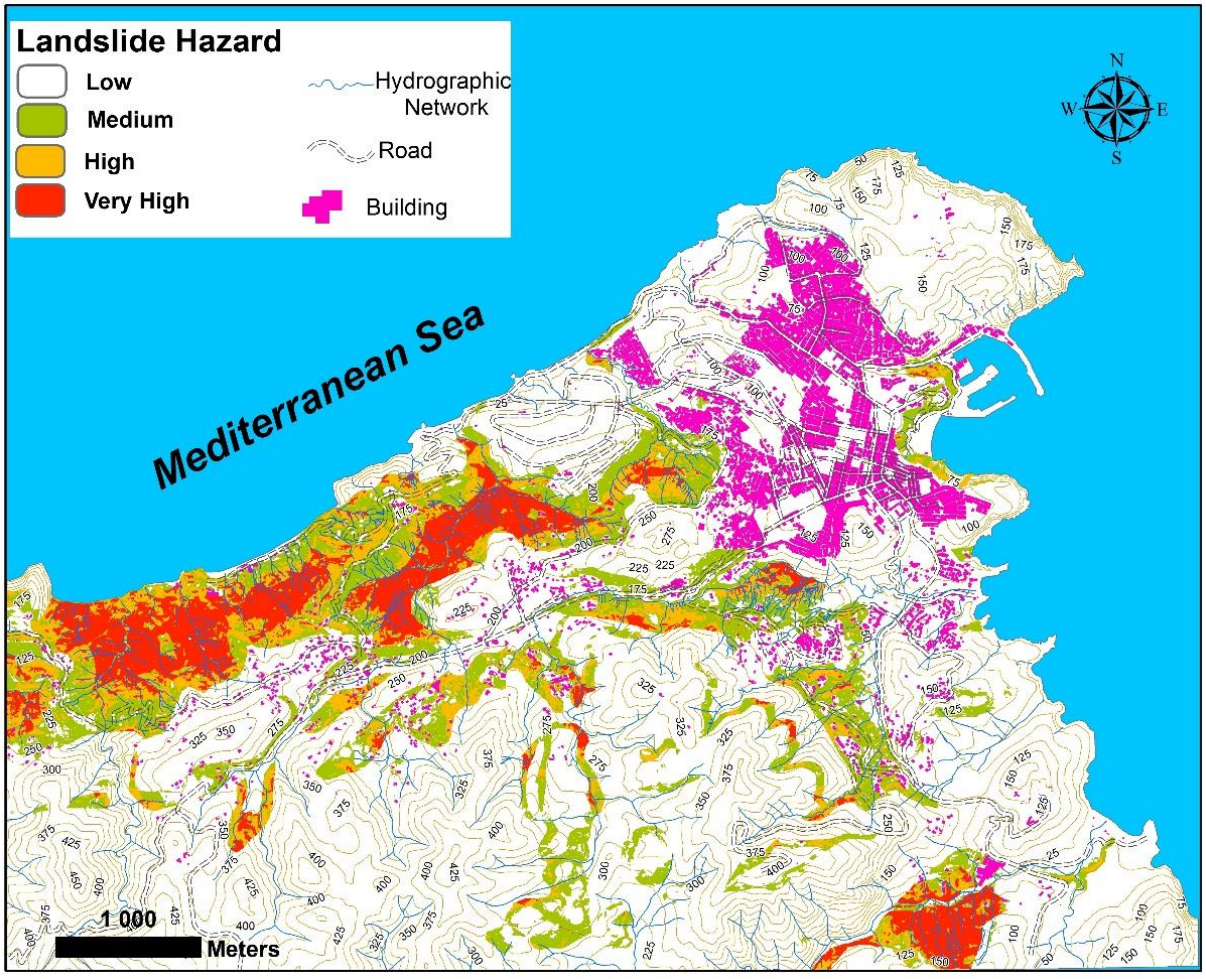

Figure 10: Landslide susceptibility map derived from the model 11 probability map.

DISCUSSION AND CONCLUSION

The landslide susceptibility modeling using the evidence theory gives very satisfactory objective results compared to other qualitative methods (Fares(1994); Margaa (1994)). The latter methods are of great interest in selecting a number of determining factors and defining their individual contributions to landslide movement.

However, they have certain limitations, especially at threshold levels and the prioritization of each of the determining factors in relation to its relative importance in the genesis of ground motion. Thus, qualitative judgement of the obtained results from different levels of hazard (high, moderate, low) without any quantification of these terms. However, the evidence theory method currently used by several authors (Pradhan et al., 2010; Mohammady et al., 2012; Devkota et al., 2013; Dumlao & Victor, 2015; Ozdemir & Altural, 2013; Vakhshoori & Zare, 2016; Bai et al., 2010; Mastere, 2011) has given quantitative results based on the coupling between statistical and probabilistic models. It allows the calculation of positive or negative weights for each causative factor and the determination of combinations of factors generating landslides in the study area. Thus, the use of the ROC curve allows to validate the results and to choose the model with the right prediction capacity.

The factors identified in this study all have a strong correlation with landslides occurred. The results show that geological conditions: lithology and faults can have a positive influence on the initiation of landslides. For example, as the results show, landslides are concentrated in lithology dominated by marls, or shales, or by red clays and sandstones and also close to the faults. The last result is confirmed in the field by numerous landslides observed at the nearby of the Ajdir active fault (Poujol et al., 2014) crossing Al Hoceima. In addition, the hydrographic network and steep slopes constitute a significant effect on the occurrence of these phenomena. They are followed by the moderate influence of other factors: such as anthropic action and seismic microzoning which have a moderate effect on the occurrence of these events.

Comparison of the results of the AUC of the different combinations allowed me to identify the best simulations obtained, these are the combinations 'M1', AUC=0.899; 'M8', AUC = 0.90; 'M11', AUC=0.902 and 'M12', AUC=0.897. It can be seen that the tests integrating the predictive neo-variables have improved the predictive capacity of the model. The AUC value of combination 11 allowed to deduce that the neo-predictive variables contribute to the improvement of the predictive potential of the model.. The combination of the inventoried landslides with the a posteriori probability map (susceptibility map) allows to classify the majority of the observed landslide grids in high and very high hazard classes (69% of the observed landslides fall into high and very high susceptibility classes). These areas are mainly located within the old landslides of large magnitude marked by important landslides and strong regressive erosion, highlighting the very advanced degree of surface degradation.

The preferred map has a more accurate hazard zonation. It is based on the main instability factors affecting the entire study area. The lithological nature, the structure and shape of the slope, and the topography, create the conditions for movement, which is triggered by heavy rainfall or by seismic activities with various modalities depending on land use and anthropogenic activities. It is a kind of exploratory document, likely to help especially in the context of risk prevention. Examination of the obtained map shows that the areas with high and very high hazard (frequent to very frequent landslides) are related to valleys and essentially to the level of schistose and marl formations. These zones are generally characterized by low cohesion, steep slope, clay intercalations, intense fracturing. These sectors are considered non-constructible. Those noted of average hazard (rather frequent landslides) are likely to be developed on condition that unstable landslides are stabilized and gullies are corrected by systems of thresholds and benches. For low or no-hazard zones (non-existent landslides

or exceptional occurrences), the risks of instability are low, and their development does not a priori pose any constraint.

The obtained results show that the model chosen in this study performs satisfactorily. However, I don't forget that the obtained results in this work can be improved if some data that have a direct relation with the occurrence of landslides in the study area are available, such as: rainfall data, geotechnical data and hydrogeological data, distributed over the whole study area. On the other hand, if a large-scale lithological map of the study area is available, allowing the petrographic definition of intermediate rocks that are not defined in the current geological map of Al Hoceima (scale 1/50000). It is recommended to include these data sets into the analysis in order to examine all the mechanisms and the factors that influence instability.

ACKNOWLEDGMENTS

The author highly acknowledges all the individuals who were consulted during the study

REFERENCES

Andrieux, J. 1971. La structure du Rif central, étude des relations entre la tectonique de compression et les nappes de glissement dans un tronçon de la chaîne alpine. – *Notes et Mém. Serv. Géol. Maroc*, n° 235, 155 p.

Azzouz O. (1992) – Lithostratigraphie et tectonique des terrains paléozoïques ghomarides du massif des Bokoya (Rif Interne, Maroc). – Thèse 3e cycle, Rabat, 208 p.

Azzouz, O., El Fellah, B., et CHalouan, A. 2002. Processus de glissement dans le Massif de Bokoya (Rif interne, Maroc) : exemple de Cala Bonita. Bulletin de l'Institut scientifique. 24 : 33-40. Disponible à l'adresse http://www.israbat.ac.ma/.

Bai, SB., Wang, J., Lü, GN., Zhou, PG., Hou, SS., et Xu, SN. 2010. GIS-based logistic regression for landslide susceptibility mapping of the Zhongxian segment in the Three Gorges area, China. Geomorphology. 115(1),23-31.Doi: 10.1016/j.geomorph .2009.09.025.

Beguería, S. 2006. Validation and Evaluation of Predictive Models in Hazard Assessment and Risk Management. Natural Hazards. 37(3), 315-329. Doi: 10.1007/s11069-005-5182-6.

Bonham-Carter, GF. 1994. Geographic Information Systems for Geoscientists: modelling with GIS. Pergamon Press, Ottawa, pp.302-328.

Bui, D. T., Lofman, O., Revhaug, I., et Dick, O. 2011. Landslide susceptibility analysis in the Hoa Binh province of Vietnam using statistical index and logistic regression. Natural Hazards. 59(3), 1413-1444. doi: 10.1007/s11069-011-9844-2.

Carrara, A. 1983. Multivariate models for landslide hazard evaluation. Journal of the International Association for Mathematical Geology, 15(3),403-426. doi: 10.1007/bf01031290.

Corominas, J., van Westen, C., Frattini, P., Cascini, L., Malet, J.-P., Fotopoulou, S., Smith, et J. T. 2014. Recommendations for the quantitative analysis of landslide risk. Bulletin of Engineering Geology and the Environment, 73(2), 209-263. doi: 10.1007/s10064-013-0538-8.

Dai, F., et Lee, C.2002. Landslide characteristics and slope instability modeling using GIS, Lantau Island, Hong Kong. Geomorphology, 42(3), 213-228. doi:10.1016/S0169-555X(01)00087-3.

Devkota, K. C., Regmi, A. D., Pourghasemi, H. R., Yoshida, K., Pradhan, B., Ryu, I. C., et Althuwaynee, O. F. 2013. Landslide susceptibility mapping using certainty factor, index of entropy and logistic regression models in

GIS and their comparison at Mugling–Narayanghat road section in Nepal Himalaya. Natural Hazards, 65(1), 135-165. doi: 10.1007/s11069-012-0347-6.

Dumlao, A., et Victor, J. 2015. GIS-aided Statistical Landslide Susceptibility Modeling And Mapping Of Antipolo Rizal (Philippines). Paper presented at the IOP Conference Series: Earth and Environmental Science 26 (2015) 012031. doi:10.1088/1755-1315/26/1/012031.

ESRI, 2016. ArcGIS Desktop : version 10.6. Institut de recherche sur les systèmes environnementaux, Redlands, Californie, Etats-Unis.

Ezzine, H., Merrouni, F. E., et Mansour, M**.** 2008. Modélisation probabiliste de la susceptibilité aux mouvements de terrain par la théorie de l'évidence. Cas du contexte complexe du Rif Marocain. GEO OBSERVATEUR, Numéro 17, 47-63.

Fares, A., Rollet, M., et Broquet, P.1994. Méthodologie de la cartographie des risques naturels liés aux mouvements de terrain. Revue française de géotechnique. 69, 63-72. Doi :10.1051/geotech/1994069063.

Fressard, M. 2013. Les glissements de terrain du Pays d'Auge continental (Normandie, France) Caractérisation, cartographie, analyse spatiale et modélisation. Thèse de doctorat,*Laboratoire LETG - Caen - Géophen UMR 6554 CNRS.*Université de Caen Basse-Normandie. 332p.

Gorsevski, P. V., Donevska, K. R., Mitrovski, C. D., et Frizado, J. P. 2012. Integrating multi-criteria evaluation techniques with geographic information systems for landfill site selection: a case study using ordered weighted average. Waste Manag, 32 (2), 287-296. doi: 10.1016/j.wasman.2011.09.023.

Kim, H. Y., 2017. Statistical notes for clinical researchers: Chi-squared test and Fisher's exact test. Restor Dent Endod. 42(2):152-155. https://doi.org/10.5395/rde.2017.42.2.152

Labriki, A., Chakiri, Nouaim, W., Allouza, M., Bejjaji, Z., & Ezzayani, J. 2017.Etude Géotechnique Et Modélisation Volumique Des Zones Instables ; Processus D'effondrement De La Falaise Adjacente À La Voie De Contournement Du Port d'Al Hoceima (Rif, Maroc) *European Scientific Journal, ESJ*, *13*(9), 251. https://doi.org/10.19044/esj.2017.v13n9p251

Labriki, A., Chakiri, S., Razoki, B., Bejjaji, Z., El Hmidi, F. & Kaid Rassou, K**.** 2019. Study of the geo-mechanical evolution of the Paleozoic massif of Al Hoceima's tectonic klippe, by analyzing the instability structures and the interpretation of geotechnical data (Rif, Morocco). Bulletin de l'Institut Scientifique, Rabat, Section Sciences de la Terre, 41, 13 – 23

Lee, S. 2005. Application of logistic regression model and its validation for landslide susceptibility mapping using GIS and remote sensing data. International Journal of Remote Sensing, 26(7), 1477-1491. doi: 10.1080/01431160412331331012.

Margaa, K., et Abdelgader, A. 1998. Une méthodologie de cartographie des zones potentiellement instables Application à la région d'Al Hoceima (Maroc). Canadian geotechnical journal, 35(3), 460-470. doi: 10.1139 / cgj-35-3-460.

Mastere, M. 2011. La susceptibilité aux mouvements de terrain dans la province de Chefchaouen (Rif Central, Maroc) : Analyse Spatiale, Modélisation Probabiliste Multi-Echelle & Impacts sur l'Aménagement et l'Urbanisme. Thèse de doctorat. Université de Bretagne occidentale. 296p. Disponible à l'adresse : https://tel.archives-ouvertes.fr/tel-00679623.

Maurer, G. (1968). Les montagnes du Rif central : étude géomorphologique (Vol. 14): Rabat, Maroc: Institut scientifique chérifien, Ministère de l'éducation nationale et des baux-arts, Royaume du Maroc.

Mégard, F. 1963. La partie orientale du massif des Bokoya : études géologiques. Thèse de doctorat, Université de Pierre et Marie Curie. Paris, 111p.

Mezughi, T., Akhir, J. M., Rafek, A. G., & Abdullah, I. 2011. A multi-class weight of evidence approach for landslide susceptibility mapping applied to an area along the E–W highway (Gerik–Jeli), Malaysia. EJGE, 16, 1259-1273. Disponible à l'adresse : https://ukm.pure.elsevier.com/en/publications/a-multi-class-weight-of-evidence-pproach-for-landslide-susceptib.

Millies-Lacroix, A**.** (1968). Les glissements de terrains. Présentation d'une carte prévisionnelle des mouvements de masse dans le Rif (Maroc septentrional). Mines et Géologie, 27, 45-55.

Mohammady, M., Pourghasemi, H. R., & Pradhan, B. 2012. Landslide susceptibility mapping at Golestan Province, Iran: a comparison between frequency ratio, Dempster–Shafer, and weights-of-evidence models. Journal of Asian Earth Sciences, 61, 221-236. doi:10.1016/j.jseaes.2012.10.005.

Mourier T. (1982) – Etude géologique et structurale du massif des Bokoya. – *Trav. Lab. Géol. de l'Afrique*, 6, Univ. Paris Sud.

Neuhäuser, B., & Terhorst, B. 2007. Landslide susceptibility assessment using "weights-of-evidence" applied to a study area at the Jurassic escarpment (SW-Germany). Geomorphology, 86(1), 12-24. doi:10.1016/j.geomorph.2006.08.002.

Ozdemir, A., & Altural, T. 2013. A comparative study of frequency ratio, weights of evidence and logistic regression methods for landslide susceptibility mapping: Sultan Mountains, SW Turkey. Journal of Asian Earth Sciences, 64, 180-197. doi:10.1016/j.jseaes.2012.12.014.

Pimiento Chamorro, E. 2010. Shallow landslide susceptibility: modelling and validation. Thèse de doctorat. Département de géographie physique et de science des écosystèmes. Université Ehime, Japon. Disponible à l'adresse http://lup.lub.lu.se/student-papers/record/3559066.

Poujol A., Ritz J.-F., Tahayt A., Vernant P., Condomines M., Blard P.-H., Billant J., Vacher L., Hni L., Koulali Idrissi A. (2014). Morphotectonics of the Rif region (Morocco): New insights on its present-day kinematics. Journal of Geodynamics, Volume 77, pg 70–88, DOI:10.1016/j.jog.2014.01.004.

Pradhan, B., Oh, H.-J., et Buchroithner, M. 2010. Weights-of-evidence model applied to landslide susceptibility mapping in a tropical hilly area. Geomatics, Natural Hazards and Risk, 1(3), 199-223. doi: 10.1080/19475705.2010.498151.

Regmi, N. R., Giardino, J. R., et Vitek, J. D. 2010. Modeling susceptibility to landslides using the weight of evidence approach: Western Colorado, USA. Geomorphology, 115(1–2), 172-187. https:/doi.org/10.1016/j.geomorph.2009.10.002.

Reza Pourghasemi, Hamid & Goli Jirandeh, Abbas & Pradhan, Biswajeet & Xu, Chong & Gokceoglu, Candan. 2013. Landslide susceptibility mapping using support vector machine and GIS at the Golestan Province, Iran 2. Journal of Earth System Science. 122. doi :10.1007/s12040-013-0282-2.

Spiegelhater, D., Kill-Jones, R.P., 1984. Statistical and knowledge approachesto clinical decision-support systems, with an application in gastroenterology. Journal of the Royal Statistical Society, 147, 35-77.

Talhaoui, A., Iben Brahim, Aberkan, H., Kasmi, M., et Mouraouah, A. 2004. seismic microzonation and site effects at al hoceima city, morocco. Journal de génie parasismique, 8 (4) :585-596. DOI: 10.1080 / 13632460409350502.

Thiery, Y.2007. Susceptibilité du Bassin de Barcelonnette (Alpes du sud, France) aux mouvements de versant : cartographie morphodynamique, analyse spatiale et modélisation probabiliste. Thèse de doctorat. Département *Géographie Physique et Environnement.* Université de Caen. 445p. Disponible à l'adresse https://tel.archives-ouvertes.fr/tel-00259135.

Thiery, Y., Malet, J. P., Sterlacchini, S., Puissant, A., & Maquaire, O. (2007). Landslide susceptibility assessment by bivariate methods at large scales: Application to a complex mountainous environment. *Geomorphology*, *92*(1–2), 38-59. doi: https://doi.org/10.1016/j.geomorph.2007.02.020

Thiery, Y., Sterlacchini, S., Malet, J.-P., Puissant, A., et Maquaire, O. 2004. Modélisation spatiale de la susceptibilité des versants aux mouvements de terrain. Paper presented at the Conférence CASSINI-SIGMA 2004: Géomatique et Analyse Spatiale, Grenoble, p. 1-13.

Vakhshoori, V., & Zare, M. 2016. Landslide susceptibility mapping by comparing weight of evidence, fuzzy logic, and frequency ratio methods. Geomatics, Natural Hazards and Risk, 7(5), 1731-1752. doi: 10.1080 / 19475705.2016.1144655.

Van Den Eeckhaut, M., Reichenbach, P., Guzzetti, F., Rossi, M., & Poesen, J. 2009. Combined landslide inventory and susceptibility assessment based on different mapping units: an example from the Flemish Ardennes, Belgium. Natural Hazards and Earth System Sciences, 9(2), 507-521. Doi:10.5194/nhess-9-507-2009.

Van Westen, C. J. 1993. Application of geographic information systems to landslide hazard zonation. Ph-D Dissertation, Technical University Delft. ITC-PublicationNumber 15, ITC, Enschede, The Netherlands, pp. 160-167.

Yalcin, A., Reis, S., Aydinoglu, A., & Yomralioglu, T. 2011. A GIS-based comparative study of frequency ratio, analytical hierarchy process, bivariate statistics and logistics regression methods for landslide susceptibility mapping in Trabzon, NE Turkey. Catena, 85(3), 274-287. doi: 10.1016/j.catena.2011.01.014.